AGU PUBLICATIONS

JGR

Journal of Geophysical Research: Space Physics

BRIEF REPORT

10.1002/2013JA019551

Key Points:

- Solar wind pressure pulse-driven vortex was observed in the magnetosphere
- Simulation and ground magnetic field data confirm this tailward moving vortex
- The vortex can penetrate deep inside the tail plasma sheet and couple to FLRs

Supporting Information:

- Readme
- Animation S1

Correspondence to:
Q. Q. Shi,
sqq@pku.edu.cn

Citation:
Shi, Q. Q., et al. (2014), Solar wind pressure pulse-driven magnetospheric vortices and their global consequences, *J. Geophys. Res. Space Physics*, *119*, 4274–4280, doi:10.1002/2013JA019551.

Received 22 OCT 2013
Accepted 27 MAY 2014
Accepted article online 6 JUN 2014
Published online 24 JUN 2014

Solar wind pressure pulse-driven magnetospheric vortices and their global consequences

Q. Q. Shi[1,2], M.D. Hartinger[3], V. Angelopoulos[2], A.M. Tian[1], S.Y. Fu[4], Q.-G. Zong[4], J. M. Weygand[2], J. Raeder[5], Z.Y. Pu[4], X.Z. Zhou[2], M.W. Dunlop[6], W.L. Liu[7], H. Zhang[8], Z.H. Yao[4], and X.C. Shen[1]

[1]Shandong Provincial Key Laboratory of Optical Astronomy and Solar-Terrestrial Environment, School of Space Science and Physics, Shandong University, Weihai, China, [2]Earth, Planetary and Space Sciences Department, University of California, Los Angeles, California, USA, [3]Atmospheric, Oceanic, and Space Sciences Department, University of Michigan, Ann Arbor, Michigan, USA, [4]School of Earth and Space Sciences, Peking University, Beijing, China, [5]Space Science Center and Physics Department, University of New Hampshire, Durham, New Hampshire, USA, [6]Space Sciences Division, SSTD, Rutherford Appleton Laboratory, Didcot, UK, [7]Space Science Institute, School of Astronautics, Beihang University, Beijing, China, [8]Institute of Geology and Geophysics, Chinese Academy of Sciences, Beijing, China

Abstract We report the in situ observation of a plasma vortex induced by a solar wind dynamic pressure enhancement in the nightside plasma sheet using multipoint measurements from Time History of Events and Macroscale Interactions during Substorms (THEMIS) satellites. The vortex has a scale of 5–10 *Re* and propagates several *Re* downtail, expanding while propagating. The features of the vortex are consistent with the prediction of the Sibeck (1990) model, and the vortex can penetrate deep (~8 *Re*) in the dawn-dusk direction and couple to field line oscillations. Global magnetohydrodynamics simulations are carried out, and it is found that the simulation and observations are consistent with each other. Data from THEMIS ground magnetometer stations indicate a poleward propagating vortex in the ionosphere, with a rotational sense consistent with the existence of the vortex observed in the magnetotail.

1. Introduction

Flow vortices are common in ordinary fluids. In a plasma, they also exist but their structure and evolution are complicated by the presence of electric and magnetic fields. Plasma vortices can transport plasma across boundaries [e.g., *Miura*, 1984; *Hasegawa et al.*, 2004]. They can also generate field-aligned currents (FACs) and contribute to the aurora [e.g., *Birn et al.*, 2004; *Keiling et al.*, 2009; *Lui et al.*, 2010]. Vortices on different scales have been found in the heliosphere [*Burlaga*, 1990], the Earth's ionosphere, and the magnetosphere under different external or internal conditions [e.g., *Hones et al.*, 1978; *Friis-Christensen et al.*, 1988; *Glassmeier et al.*, 1989; *Lyatsky et al.*, 1999; *Murr et al.*, 2002; *Motoba et al.*, 2003; *Sibeck et al.*, 2003; *Sundkvist et al.*, 2005; *Juusola et al.*, 2010; *Tian et al.*, 2010].

Many previous observations of plasma flow vortices have been made at the dayside ionosphere based on ground magnetic field or SuperDarn radar observations [e.g., *Friis-Christensen et al.*, 1988; *Glassmeier et al.*, 1989; *Yahnin et al.*, 1996; *Lyatsky et al.*, 1999; *Motoba et al.*, 2003; *Murr et al.*, 2002; *Sibeck et al.*, 2003; *Juusola et al.*, 2010]. Nightside magnetospheric vortex observations have also been reported [e.g., *Hones*, 1978; *Hasegawa et al.*, 2004; *Keiling et al.*, 2009; *Lui et al.*, 2010; *Tian et al.*, 2010] and simulated [*El-Alaoui et al.*, 2010; *Wang et al.*, 2010; *Sun et al.*, 2011, 2012; *Shi et al.*, 2013; *Samsonov and Sibeck*, 2013], but we are not aware of any clear in situ observations of such vortices attributed to by solar wind pressure enhancements either in the dayside or nightside plasma sheet. *Wang et al.* [2010] and *Sun et al.* [2011, 2012] looked at the response of the nightside magnetotail to a pressure increase and examined the magnetic field response using a global MHD simulation and comparative GOES/THEMIS/Double Star data. Although they did not explicitly report it, a vortex was clearly seen in their simulation. Observational evidence of such a sudden impulse (SI)-associated vortex is still lacking. *Sibeck* [1990] proposed an interaction model between solar wind pressure pulses and the magnetosphere, in which a single- or double-vortex structure inside the magnetosphere near the magnetopause, with a concomitant ionospheric signature was predicted. The ionospheric counterpart was later observed using SuperDarn radar and ground magnetometers [e.g., *Sibeck et al.*, 2003]; however, there are still no in situ observations of solar wind dynamic pressure-induced vortices near the magnetopause and the adjacent tail plasma sheet.

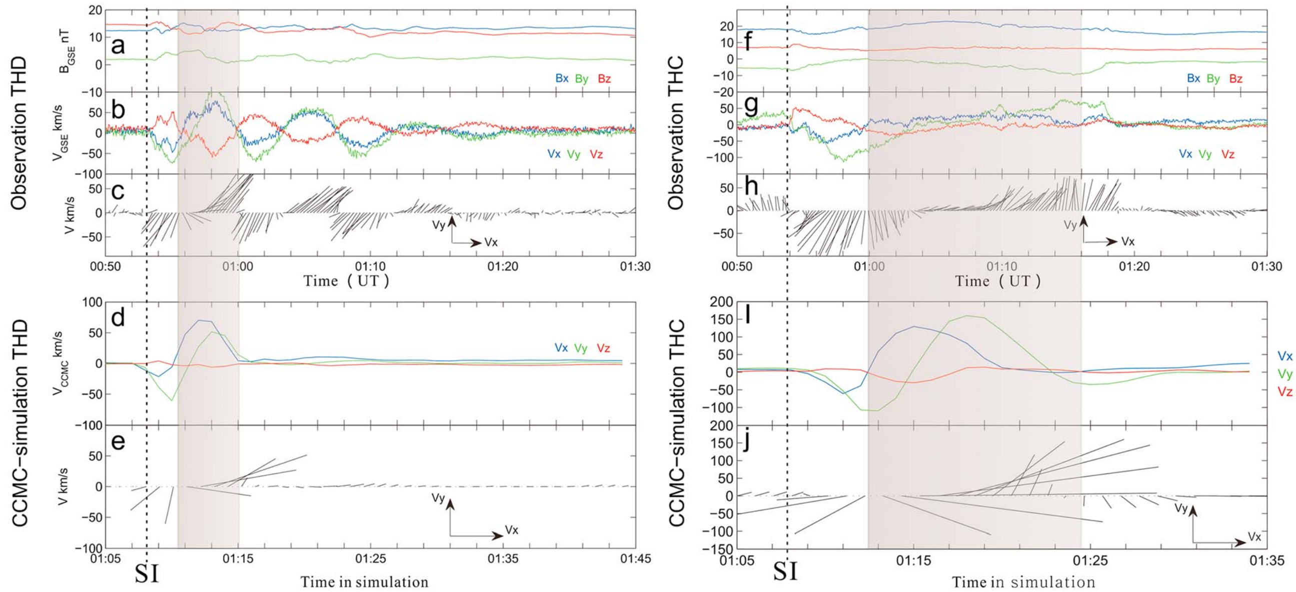

Figure 1. THEMIS observations of the magnetotail response to the solar wind pressure pulse and global MHD simulation result. The time corresponding to the vortex passage is illustrated in the shaded region. The vertical lines indicate the SI start time/solar wind dynamic pressure pulse arrival time. (a) magnetic field observed by THD. (b) Ion velocity observed by THD. (c) Ion velocity vector in *xy* plane in GSE. (d) Simulated ion velocity at THD position in the simulation domain. (e) Simulated ion velocity vector in *xy* plane at THD position. (f)–(j). Same as Figures 1a–1e but for THC.

Recently, *Shi et al*. [2013] reported standing Alfvén waves in the nightside plasma sheet after SIs. They proposed that those are field line resonances (FLRs) driven by the solar wind dynamic pressure enhancements through a pressure-induced vortex at the boundary. The authors suggested this as a new mechanism for FLR excitation. They proposed that where the vortex perturbation frequency matches the local standing Alfvén wave frequency, an FLR will be excited. The ULF response to the vortex structure induced by an SI is different from the direct response to the SI. In the former case, the spatial structure and propagation of the vortex can lead to a frequency selection, exciting standing Alfven waves at discrete frequencies and locations. In the latter case, a broadband frequency response is expected, since the SI contains rapid step-like (or spiky) variations in the time domain. Analysis of the magnetospheric response to the SI in the time domain—in particular, identification of vortex structures using in situ observations—is required to confirm the operation of either ULF wave excitation mechanism in the nightside magnetosphere. Although vortices can be found in simulations [e.g., *Samsonov and Sibeck*, 2013; *Shi et al*., 2013] after an SI, until now no direct evidence of such vortices has been reported from in situ observations. In this paper, we report the first in situ observation of such vortices attributed to solar wind dynamic pressure pulse in the nightside plasma sheet using coordinated observations from multiple THEMIS satellites. Global MHD simulations and ground magnetometer measurements are also performed to confirm the finding.

2. Observations and Global MHD Simulations

On 24 April 2009, the Wind satellite detected an interplanetary shock (see Figure 8 in *Shi et al*. [2013]) with a dynamic pressure increase from ~0.7 to 1.7 nPa. In response, THEMIS B, C, and D in the dusk magnetotail observed magnetic field and ion velocity perturbations after the SI at ~00:53 UT, as shown in Figure 1 for THEMIS C and D where the vertical lines indicate the SI start time/solar wind dynamic pressure pulse arrival time. In this case THEMIS D was separated from B and C by about 4 *Re* along *X*, and THEMIS B and C were separated by about 1.8 *Re* along the *Y* direction, as shown in Figure 2b (all coordinates are in the GSE coordinate system). The velocity vectors versus time as shown in Figures 1c and 1h are consistent with motion through a typical vortex, as exemplified by trajectory 3 in Figure 7 of *Keiling et al*. [2009]. The shaded areas correspond to the vortex proper, while the time between the SI start time (vertical lines) and the shaded area indicates a tailward flow response after the lateral compression of the magnetosphere by the solar wind dynamic pressure enhancement which has been studied in *Shi et al*. [2013].

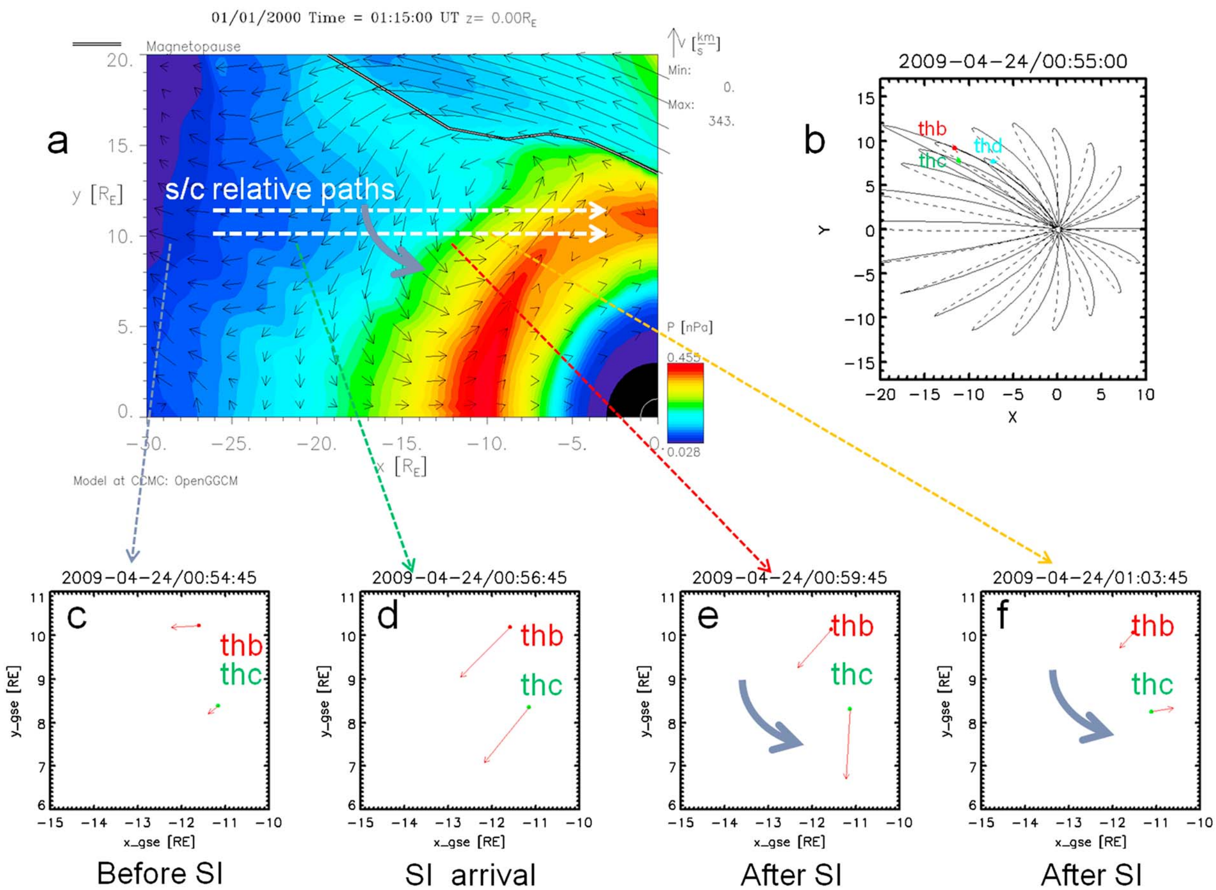

Figure 2. Comparison of vortex perturbations corresponding to rotation as observed by THEMIS B and C with MHD simulation results. (a) The global MHD simulation results shown in duskside. The background color indicates plasma pressure, and the arrows represent the plasma velocities. (b) THEMIS probe potions for satellite B, C, and D. (c–d) Plasma velocity vectors observed by THEMIS B and C at different moments.

We have carried out a global MHD simulation through the Community Coordinated Modeling Center (CCMC) using the OpenGGCM MHD code [*Raeder et al*., 2008] to simulate this kind of solar wind pressure pulse/magnetosphere interaction. The solar wind input parameters for the MHD simulations before (after) the solar wind pressure are 4.0 n/cm^3 (7 n/cm^3) for density, [320,0, 0] km/s ([380, 0, 0] km/s) in GSE for solar wind velocity, and [0, 3, 3] nT ([0, 7, 5] nT) in GSE for the interplanetary magnetic field (IMF). Both at the dawn and dusk sides of the magnetotail a tailward moving single vortex can be found in the simulation result. Here we only show the dusk part of the magnetotail in Figure 2a. An animation can be seen in the supporting information (Note that the default time of the model simulation in CCMC starts from 2001, which does not correspond to the real time of the observation.). We plot the time series of the plasma velocities/vectors at (−7.2, 7.7, 0.0) *Re* (corresponding to THEMIS D position) and (−11.1, 8.3, 0.0) *Re* (corresponding to THEMIS C position) in the simulation domain in Figures 1d/1e and 1i/1j, respectively. The shaded areas in Figure 1 correspond to the simulated vortex in Figure 2. It can be seen that the velocity vectors observed by THEMIS are consistent with those simulated by the MHD model.

The vortex was followed at THD's position by field line oscillations. The vortex continued moving tailward and was later observed by THB and THC which were 4 *Re* away from THD. *Shi et al*. [2013] have studied the wave activity observed by THD after the time corresponding to the shaded area in the left-hand panel of Figure 1. They found that it was a standing Alfvén wave consistent with an FLR and proposed that the wave was driven by a passing vortex driven by the solar wind SI. The ensuing standing Alfvén wave activity is not captured well by the MHD simulations, perhaps due to the simulation accuracy or due to the boundary condition settings at the ionosphere. The vortex is the topic of this report.

 10.1002/2013JA019551

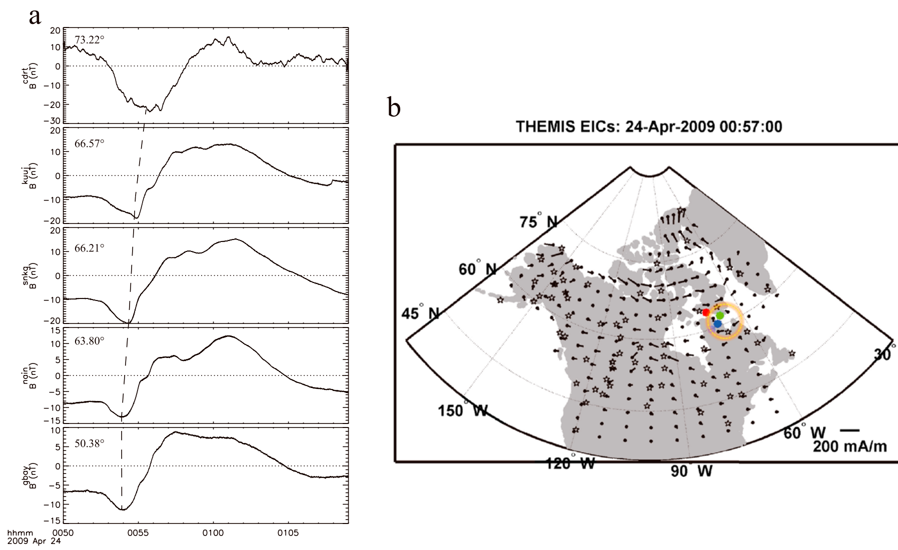

Figure 3. (a) *H* component of the transient magnetic variation recorded at stations near the foot points of THEMIS B, C, and D. (b) Equivalent ionospheric currents (EICs). The stars indicate the ground stations and the solid circles indicate the foot points of THEMIS B (red), C (green), and D (cyan). The vectors indicate the current direction and intensity. The yellow circle highlights the vortex position.

Two of our satellites (THB and C) were downtail of THD and separated mostly along *Y* by about 1.5 *Re*. We can therefore plot the flow vectors at every moment, as shown in Figures 2c–2f and compare the observed velocities to what is expected from simulations of a passing vortex. Before the SI (Figure 2c), we find that the flow vectors observed by THB and C are very small. Upon arrival of the SI (Figure 2d), we find tailward flows from both THB and C, consistent with a lateral compression of the magnetopause. Several minutes later, the flow vectors at THB and C become quite different from each other (Figures 2e and 2f), and the sense of rotation is consistent with counterclockwise motion, as seen in the simulation (Figure 2a) and as expected from the *Sibeck* [1990] model. Therefore, from simulation and multipoint observations, we confirm that this is a tailward moving vortex that is caused by magnetospheric compression by the solar wind dynamic pressure enhancement.

From simulations and observations we also notice that the vortex is deep inside the magnetosphere, rather than simply near the magnetopause, since THC is ~8 *Re* from the statistical location of the magnetopause boundary under these dynamic pressure conditions ([*Shue et al*., 1998], with $P_{dyn} = 2$ nPa; $B_z = 1$ nT). According to the simulation the inner edge of the vortex is near $Y = 5$ *Re*. From the simulation, the scale of the vortex appears to be 5–10 *Re*, which is consistent with our observations (Our MHD simulation results are also similar to the simulation results of *Wang et al*. [2010] and *Sun et al*. [2011, 2012]). From both simulation and observations it appears that the size of the vortex is growing while propagating tailward.

From approximately 0052 UT transient magnetic variations in the *H* component were observed by THEMIS ground stations along a latitude profile near the foot points of the THEMIS satellites, as shown in Figure 3a. The bipolar signature in the *H* component is consistent with observations of traveling convection vortices by *Friis-Christensen et al*. [1988] and *Glassmeier et al*. [1989]. The time shift of the negative peak indicates a poleward propagation of the transient and is consistent with the observed tailward propagation of the driver in the magnetosphere. Figure 3b shows equivalent ionospheric currents (EICs) derived from the ground magnetic disturbance of ground magnetometer arrays (CANMOS, CARISMA, GIMA, MACCS, THEMIS, DTU, STEP, and USGS) at 00:57 UT (see *Weygand et al*. [2011] and *Keiling et al*. [2009] for a description of these techniques). A single vortex with counterclockwise rotation is seen near the ionospheric footpoints of THEMIS B, C, and D and is demarcated by a circled area in Figure 3b. The sense of rotation of the equivalent ionospheric Hall current has a divergence that is consistent with an upward FAC from current continuity [e.g., *Birn et al*., 2004; *Keiling et al*., 2009; *Yao et al*., 2012], consistent with the FAC generation by the magnetospheric flow vortex that we observed in the magnetotail.

3. Summary and Discussions

In this paper we report in situ and ground observations of a solar wind dynamic pressure enhancement-induced vortex in the nightside plasma sheet and reproduce the in situ signature using global MHD simulations. Simulation and observations consistently show a vortex driven by a sudden impulse in the solar wind and extending deep inside the magnetosphere, not only near the magnetopause.

The depth of penetration of the vortex into the tail (and the excitation of field line resonance) indicates that the energy coupling between the solar wind and the magnetosphere/ionosphere is significant. Other events (e.g., events on 28 May 2008 and 28 May 2009) from THEMIS single satellite data show that this response of the nightside plasma sheet to solar wind dynamic pressure enhancement is rather common.

At THD's position the vortex was followed by the field line oscillations after it passed. Thus, the magnetic field response in the plasma sheet to an interplanetary shock/pressure change is not always a smooth increase or decrease, sometimes there are persistent perturbations. This vortex continued propagating toward the tail and was later observed by THB and THC at a location 4 *Re* away from THD. From the simulation results we find that there is no net plasma transport; however, the front/phase of the vortex perturbation in the magnetotail plasma sheet is moving tailward—see Animation S1 in the supporting information. The response of the plasmas at different locations makes the plasma velocity vectors form a vortex-like picture as a whole. When the perturbations move tailward, the vortex also moves tailward. According to the *Sibeck* [1990] model, the compression and recovery of the field lines lead to a vortex formation. If the timing of this compression and recovery (or the timing of this vortex) matches the local field line frequency, then an FLR can be excited as suggested by *Shi et al*. [2013] and then we see more than one period of the wave, while at other places where the local field line frequency does not match the FLR the waves damp very fast. The ULF wave and the vortex are excited at the same time, and they actually may be the same feature observed with different methods: the wave is seen locally while the vortex requires a global view. The observations herein are not unique as mentioned above. *Shi et al*. [2013] have also discussed several formation mechanisms of the FLRs other than vortex, such as surface waves at the magnetopause driven by the Kelvin-Helmholtz instability [e.g., *Chen and Hasegawa*, 1974; *Southwood*, 1974; *Claudepierre et al*., 2008], cavity/waveguide modes [e.g., *Kivelson and Southwood*, 1985, *Walker et al*., 1992; *Rickard and Wright*, 1994, 1995], and direct excitation by a solar wind pressure pulse [e.g., *Samson and Rostoker*, 1972; *Waters et al*., 1995]. We found that none of these mechanisms could explain the ULF wave observations. Since there are no obvious density and pressure fluctuations the generation mechanism described by *Kepko et al*. [2002] (also seen in *Claudepierre et al*. [2010]) is also not applicable here. In addition, IMF variations might also drive vortices or low-frequency waves directly [e.g., *Walker et al*., 2006; *El-Alaoui et al*., 2009; *Nedie et al*., 2012]. *Nedie et al*. [2012] have seen waves in the solar wind as variations in IMF *Bz* at the frequency of SuperDARN FLRs. For the case we present in this paper, there are some IMF fluctuations which may contribute to the vortex and FLR formation processes. We have conducted spectral analysis (not shown here) and find that the frequency of the IMF *Bx* oscillation is close to 2 mHz, which is close to the FLR frequency of this event. These IMF fluctuations may contribute to the observed wave activity—it is not possible to rule them out since the MHD simulation does not fully capture the physics of standing Alfven waves and thus cannot directly establish what causes the waves. However, we find that the IMF fluctuations start ~4 min earlier than the dynamic pressure enhancement (which coincides with the SI start time as well as the ULF wave start time). Also, for the other two events we studied in *Shi et al*. [2013], there are no such IMF oscillations, but the ULF wave start times all coincide with the SI arrival or the dynamic pressure enhancement. Thus, IMF oscillations may affect the ULF wave activity, but they are not crucial for generating the ULF waves.

A large amount of previous observations and models have discussed ionosphere traveling convection vortices, which are observed on the dayside and are also related to solar wind dynamic pressure enhancements [e.g., *Friis-Christensen et al*., 1988; *Glassmeier et al*., 1989; *Kivelson and Southwood*, 1991]. These ionospheric vortices map to the dayside or flank magnetopause or low-latitude boundary layer (LLBL) [e.g., *McHenry et al*., 1989; *Kivelson and Southwood*, 1991; *Glassmeier*, 1992]. Our in situ observations at the nightside differ significantly from those of the dayside ionospheric convection vortices and their predicted magnetospheric driver locations, since we observed the driver plasma vortex deep inside the nightside magnetosphere. The difference between dayside and nightside is likely due to the fact that the restoring force from the magnetosphere changes from being normal to the boundary at the dayside to be oblique to the boundary tailward of the terminator. At the nightside the restoring force becomes weaker, since the boundary field is weaker there and its gradient points at an angle to the magnetopause. This makes the pressure pulse on the nightside protrude farther inside the magnetosphere. Some studies have suggested that some dayside ionospheric traveling convection vortices may map to the nightside plasma sheet near the flanks [*Yahnin and Moretto*, 1996; *Yahnin et al.*, 1997]. This would not be inconsistent with our observations on the nightside, and in situ observations of these phenomena in the ionosphere and magnetosphere covering both nightside and dayside are needed.

To generate the ionosphere vortex, the *Kivelson and Southwood* [1991] model requires a deformation of the magnetopause to generate a FAC connecting to the ionosphere. *Glassmeier* [1992] suggested that the compression would perturb the magnetopause current and in turn generate the upward and downward FAC corresponding to the vortex in the ionosphere. The aforementioned models do not require an in situ vortex in the magnetosphere or near the magnetopause. The *Sibeck* [1990] model, however, considers in situ vortex near the magnetopause. According to this model, when the shock impinges the magnetopause, a fast wave will be launched inside the magnetosphere. If this fast mode wave propagates faster than the magnetosheath part of the shock, the magnetospheric field lines move outward where the fast wave arrives and then we can expect a tailward moving double vortex. If the fast mode wave inside the magnetosphere does not advance in front of the magnetosheath discontinuity, then we should only expect one single vortex. This situation should happen under northward IMF when the LLBL is thick and, in turn, the fast mode speed inside the magnetosphere is not that fast. In our observation and simulation results it appears that a single vortex is evident. This may be due to the northward IMF condition, consistent with *Sibeck*'s [1990] model. In addition, the fact that his vortex as an FAC source is deeper inside the tail, not only near the magnetopause, has not been predicted before.

In the future we need to continue data analysis in different regions, especially on the dayside, and compare with simulation and models. We plan to examine how these vortices transfer energy to waves and particles, generate aurorae, or heat the ionosphere. These studies will help us understand the effects of pressure-induced vortices and nonsteady solar wind conditions on the space environment.

Acknowledgments
We acknowledge NASA THEMIS contract NAS5-02099; J. Bonnell and F. S. Mozer for the use of the EFI data; and C. W. Carlson and J. P. McFadden for the use of the ESA data; K. H. Glassmeier, U. Auster, and W. Baumjohann for the use of FGM data provided under the lead of the Technical University of Braunschweig and with financial support through the German Ministry for Economy and Technology and the German Center for Aviation and Space (DLR) under contract 50 OC 0302. Simulation results have been provided by the Community Coordinated Modeling Center at Goddard Space Flight Center through their public Runs on Request system (http://ccmc.gsfc.nasa.gov). The CCMC is a multiagency partnership between NASA, AFMC, AFOSR, AFRL, AFWA, NOAA, NSF, and ONR. The OpenGGCM was developed by Joachim Raeder and coworkers at the University of New Hampshire. We are grateful to CDAWeb for providing the WIND data. We are grateful to Cindy Russell for help with software. This work is supported by NNSFC 41031065, 41074106, 41322031, the Shandong Natural Science Foundation JQ201112, and the Ministry of Education of China (NCET-12-0332). M.D. Hartinger was supported by NSF AGS-1230398.

Larry Kepko thanks Robert Rankin and Mostafa El-Alaoui for their assistance in evaluating this paper.

References

Amm, O., M. J. Engebretson, T. Hughes, L. Newitt, A. Viljanen, and J. Watermann (2002), A traveling convection vortex event study: Instantaneous ionospheric equivalent currents, estimation of field-aligned currents, and the role of induced currents, *J. Geophys. Res.*, *107*(A11), 1334, doi:10.1029/2002JA009472.

Birn, J. M., J. Raeder, Y. L. Wang, R. A. Wolf, and M. Hesse (2004), On the propagation of bubbles in the magnetotail, *Ann. Geophys.*, *22*, 1773–1786.

Burlaga, L. F. (1990), A heliospheric vortex street?, *J. Geophys. Res.*, *95*(A4), 4333–4336, doi:10.1029/JA095iA04p04333.

Chen, L., and A. Hasegawa (1974), A theory of long-period magnetic pulsations: 2. Impulse excitation of surface eigenmode, *J. Geophys. Res.*, *79*(7), 1033–1037.

Claudepierre, S. G., S. R. Elkington, and M. Wiltberger (2008), Solar wind driving of magnetospheric ULF waves: Pulsations driven by velocity shear at the magnetopause, *J. Geophys. Res.*, *113*, A05218, doi:10.1029/2007JA012890.

Claudepierre, S. G., M. K. Hudson, W. Lotko, J. G. Lyon, and R. E. Denton (2010), Solar wind driving of magnetospheric ULF waves: Field line resonances driven by dynamic pressure fluctuations, *J. Geophys. Res.*, *115*, A11202, doi:10.1029/2010JA015399.

El-Alaoui, M., M. Ashour-Abdalla, R. J. Walker, V. Peroomian, R. L. Richard, V. Angelopoulos, and A. Runov (2009), Substorm evolution as revealed by THEMIS satellites and a global MHD simulation, *J. Geophys. Res.*, *114*, A08221, doi:10.1029/2009JA014133.

El-Alaoui, M., M. Ashour-Abdalla, R. L. Richard, M. L. Goldstein, J. M. Weygand, and R. J. Walker (2010), Global magnetohydrodynamic simulation of reconnection and turbulence in the plasma sheet, *J. Geophys. Res.*, *115*, A12236, doi:10.1029/2010JA015653.

Farrugia, C. J., M. P. Freeman, S. W. H. Cowley, D. J. Southwood, M. Lockwood, and A. Etemadi (1989), Pressure driven magnetopause motions and attendant response on the ground, *Planet. Space Sci.*, *37*, 589.

Friis-Christensen, E., M. A. McHenry, C. R. Clauer, and S. Vennerstrom (1988), Ionospheric traveling convection vortices observed near the polar cleft: A triggered response to sudden changes in the solar wind, *Geophys. Res. Lett.*, *15*, 253–256, doi:10.1029/GL015i003p00253.

Glassmeier, K.-H. (1992), Traveling magnetospheric convection twin vortices—Observations and theory, *Ann. Geophys.*, *10*, 547–565.

Glassmeier, K.-H., M. Hönisch, and J. Untiedt (1989), Ground-based and satellite observations of traveling magnetospheric convection twin-vortices, *J. Geophys. Res.*, *94*, 2520–2528, doi:10.1029/JA094iA03p02520.

Goertz, C. K., E. Nielsen, A. Korth, K. H. Glassmeier, C. Haldoupis, P. Hoeg, and D. Hayward (1985), Observation of a possible ground signature of flux transfer events, *J. Geophys. Res.*, *90*, 4069, doi:10.1029/JA090iA05p04069.

Hasegawa, H., M. Fujimoto, T.-D. Phan, H. Rème, A. Balogh, M. W. Dunlop, C. Hashimoto, and R. TanDokoro (2004), Transport of solar wind into Earth's magnetosphere through rolled-up Kelvin-Helmholtz vortices, *Nature*, *430*, 755–758.

Hones, E. W., Jr., G. Paschmann, S. J. Bame, J. R. Asbridge, N. Sckopke, and K. Schindler (1978), Vortices in magnetospheric plasma flow, *Geophys. Res. Lett.*, *5*(12), 1059–1062, doi:10.1029/GL005i012p01059.

Juusola, L., K. Andreeova, O. Amm, K. Kauristie, S. E. Milan, M. Palmroth, and N. Partamies (2010), Effects of a solar wind dynamic pressure increase in the magnetosphere and in the ionosphere, *Ann. Geophys.*, *28*(10), 1945–1959.

Keiling, A., et al. (2009), Substorm current wedge driven by plasma flow vortices: THEMIS observations, *J. Geophys. Res.*, *114*, A00C22, doi:10.1029/2009JA014114.

Kepko, L., H. E. Spence, and H. J. Singer (2002), ULF waves in the solar wind as direct drivers of magnetospheric pulsations, *Geophys. Res. Lett.*, *29*(8), 1197, doi:10.1029/2001GL014405.

Kivelson, M. G., and D. J. Southwood (1985), Resonant ulf waves: A new interpretation, *Geophys. Res. Lett.*, *12*(1), 49–52.

Kivelson, M. G., and D. J. Southwood (1991), Ionospheric traveling vortex generation by solar wind buffeting of the magnetosphere, *J. Geophys. Res.*, *96*(A2), 1661–1667.

Lui, A. T. Y., E. Spanswick, E. F. Donovan, J. Liang, W. W. Liu, O. LeContel, and Q.-G. Zong (2010), A transient narrow poleward extrusion from the diffuse aurora and the concurrent magnetotail activity, *J. Geophys. Res.*, *115*, A10210, doi:10.1029/2010JA015449.

Lyatsky, W. B., G. J. Sofko, A. V. Kustov, D. Andre, W. J. Hughes, and D. Murr (1999), Traveling convection vortices as seen by the SuperDARN HF radars, *J. Geophys. Res.*, *104*(A2), 2591–2601, doi:10.1029/1998JA900007.

McHenry, M. A., C. R. Clauer, E. Friis-Christensen, and J. D. Kelly (1989), Observations of ionospheric convection vortices: Signatures of momentum transfer, *Adv. Space Res.*, *8*, 315–320.

Miura, A. (1984), Anomalous transport by magnetohydrodynamic Kelvin-Helmholtz instabilities in the solar wind-magnetosphere interaction, *J. Geophys. Res.*, *89*, 801–818, doi:10.1029/JA089iA02p00801.

Motoba, T., T. Kikuchi, T. Okuzawa, and K. Yumoto (2003), Dynamical response of the magnetosphere-ionosphere system to a solar wind dynamic pressure oscillation, *J. Geophys. Res.*, *108*(A5), 1206, doi:10.1029/2002JA009696.

Murr, D. L., W. J. Hughes, A. S. Rodger, E. Zesta, H. U. Frey, and A. T. Weatherwax (2002), Conjugate observations of traveling convection vortices: The field-aligned current system, *J. Geophys. Res.*, *107*(A10), 1306, doi:10.1029/2002JA009456.

Nedie, A. Z., R. Rankin, and F. R. Fenrich (2012), SuperDARN observations of the driver wave associated with FLRs, *J. Geophys. Res.*, *117*, A06232, doi:10.1029/2011JA017387.

Raeder, J., D. Larson, W. H. Li, E. L. Kepko, and T. Fuller-Rowell (2008), OpenGGCM simulations for the THEMIS mission, *Space Sci. Rev.*, *141*(1–4), 535–555.

Rickard, G. J., and A. N. Wright (1994), Alfven resonance excitation and fast wave propagation in magnetospheric waveguides, *J. Geophys. Res.*, *99*(A7), 13,455–13,464.

Rickard, G. J., and A. N. Wright (1995), Ulf pulsations in a magnetospheric waveguide: Comparison of real and simulated satellite data, *J. Geophys. Res.*, *100*(A3), 3531–3537.

Samson, J. C., and G. Rostoker (1972), Latitude-dependent characteristics of high-latitude pc 4 and pc 5 micropulsations, *J. Geophys. Res.*, *77*(31), 6133–6144.

Samsonov, A. A., and D. G. Sibeck (2013), Large-scale flow vortices following a magnetospheric sudden impulse, *J. Geophys. Res. Space Physics*, *118*, 3055–3064, doi:10.1002/jgra.50329.

Shi, Q. Q., et al. (2013), THEMIS observations of ULF wave excitation in the nightside plasma sheet during sudden impulse events, *J. Geophys. Res. Space Physics*, *118*, 284–298, doi:10.1029/2012JA017984.

Shue, J.-H., et al. (1998), Magnetopause location under extreme solar wind conditions, *J. Geophys. Res.*, *103*(A8), 17,691–17,700, doi:10.1029/98JA01103.

Sibeck, D. G. (1990), A model for the transient magnetospheric response to sudden solar wind dynamic pressure variations, *J. Geophys. Res.*, *95*(A4), 3755–3771, doi:10.1029/JA095iA04p03755.

Sibeck, D. G., N. B. Trivedi, E. Zesta, R. B. Decker, H. J. Singer, A. Szabo, H. Tachihara, and J. Watermann (2003), Pressure-pulse interaction with the magnetosphere and ionosphere, *J. Geophys. Res.*, *108*(A2), 1095, doi:10.1029/2002JA009675.

Southwood, D. (1974), Some features of field line resonances in the magnetosphere, *Planet. Space Sci.*, *22*(3), 483–491.

Sun, T. R., C. Wang, H. Li, and X. C. Guo (2011), Nightside geosynchronous magnetic field response to interplanetary shocks: Model results, *J. Geophys. Res.*, *116*, A04216, doi:10.1029/2010JA016074.

Sun, T. R., C. Wang, and Y. Wang (2012), Different *Bz* response regions in the nightside magnetosphere after the arrival of an interplanetary shock: Multipoint observations compared with MHD simulations, *J. Geophys. Res.*, *117*, A05227, doi:10.1029/2011JA017303.

Sundkvist, D., V. Krasnoselskikh, P. K. Shukla, A. Vaivads, M. André, S. Buchert, and H. Rème (2005), In situ multi-satellite detection of coherent vortices as a manifestation of Alfvénic turbulence, *Nature*, *436*, 825–828.

Tian, A. M., Q. G. Zong, Y. F. Wang, Q. Q. Shi, S. Y. Fu, and Z. Y. Pu (2010), A series of plasma flow vortices in the tail plasma sheet associated with solar wind pressure enhancement, *J. Geophys. Res.*, *115*, A09204, doi:10.1029/2009JA014989.

Walker, A., J. M. Ruohoniemi, K. Baker, R. Greenwald, and J. Samson (1992), Spatial and temporal behavior of ulf pulsations observed by the goose bay hf radar, *J. Geophys. Res.*, *97*(A8), 12,187–12,202.

Walker, R. J., M. Ashour-Abdalla, M. El Alaoui, and F. V. Coroniti (2006), Magnetospheric convection during prolonged intervals with southward interplanetary magnetic field, *J. Geophys. Res.*, *111*, A10219, doi:10.1029/2005JA011541.

Wang, C., T. R. Sun, X. C. Guo, and J. D. Richardson (2010), Case study of nightside magnetospheric magnetic field response to interplanetary shocks, *J. Geophys. Res.*, *115*, A10247, doi:10.1029/2010JA015451.

Waters, C., J. Samson, and E. Donovan (1995), The temporal variation of the frequency of high latitude field line resonances, *J. Geophys. Res.*, *100*(A5), 7987–7996.

Weygand, J. M., O. Amm, A. Viljanen, V. Angelopoulos, D. Murr, M. J. Engebretson, H. Gleisner, and I. Mann (2011), Application and validation of the spherical elementary currents systems technique for deriving ionospheric equivalent currents with the North American and Greenland ground magnetometer arrays, *J. Geophys. Res.*, *116*, A03305, doi:10.1029/2010JA016177.

Yahnin, A., and T. Moretto (1996), Travelling convection vortices in the ionosphere map to the central plasma sheet, *Ann. Geophys.*, *14*, 1025–1031.

Yahnin, A., and V. Sergeev (1996), Simultaneous satellite and ground-based observations of polar cap aurora, *Adv. Space Res.*, *18*(8), 111–114.

Yahnin, A., V. Sergeev, B. Gvozdevsky, and S. Vennerstrem (1997), Magnetospheric source region of discrete auroras inferred from their relationship with isotropy boundaries of energetic particles, in *Annales Geophysicae*, vol. 15, pp. 943–958, Springer.

Yao, Z. H., et al. (2012), Mechanism of substorm current wedge formation: THEMIS observations, *Geophys. Res. Lett.*, *39*, L13102, doi:10.1029/2012GL052055.

